PCCP

ROYAL SOCIETY OF CHEMISTRY

PAPER

Cite this: *Phys. Chem. Chem. Phys.*, 2020, **22**, 26312

Solvent-dependent termination, size and stability in polyynes synthesized *via* laser ablation in liquids†

Sonia Peggiani, Pietro Marabotti, Riccardo Alberto Lotti, Anna Facibeni, Patrick Serafini, Alberto Milani, Valeria Russo, Andrea Li Bassi and Carlo Spartaco Casari *

Received 4th August 2020,
Accepted 16th October 2020

DOI: 10.1039/d0cp04132g

rsc.li/pccp

In recent years there has been growing interest in sp-carbon chains as possible novel nanostructures. An example of sp-carbon chains is the so-called polyyne, characterized by the alternation of single and triple bonds that can be synthesized *via* pulsed laser ablation in liquid (PLAL) of a graphite target. In this work, by using different solvents in the PLAL process, *e.g.* water, acetonitrile, methanol, ethanol, and isopropanol, we systematically investigated the role of the solvent in polyyne synthesis and stability, and discussed the possible formation mechanisms. The presence of methyl- and cyano-groups in the solutions influences the termination of polyynes, allowing the detection, of hydrogen-capped polyynes up to H-C_{22}-H, methyl-capped polyynes up to H-C_{18}-CH_3 and cyanopolyynes up to H-C_{12}-CN. The assignment of each species was performed *via* UV-vis spectroscopy and supported by density functional theory simulations of vibronic spectra. In addition, surface-enhanced Raman spectroscopy allowed to highlight the differences in the shape and positions of the characteristic Raman bands of the size-selected polyynes with different terminations (hydrogen, methyl and cyano groups). The stability in time of each polyyne was investigated by evaluating the chromatographic peak area, and the effect of size, terminations and solvents on polyyne stability was individuated.

1 Introduction

Polyynes are carbon nanostructures, consisting in finite linear chains of sp-carbon atoms linked by alternated single and triple bonds, that show appealing tunability of optical and electronic properties by controlling the length of the chains and their terminations.[1,2] Polyynes are interesting not only from a technological point of view but also because they are naturally occurring in many products.[3] Moreover, they have been observed in interstellar and circumstellar media by radio-astronomy experiments detecting mainly cyanopolyynes, *via* microwave and IR spectroscopy.[4,5] Among the large variety of methods available to synthesize sp-carbon chains,[6–9] physical techniques, such as submerged arc discharge in liquid (SADL) and pulsed laser ablation in liquid (PLAL), allow to form polyynes with different lengths in a feasible way. Some papers discussed the synthesis of polyynes *via* SADL in different environments.[7,10–15] However, using PLAL, which is based on the irradiation of a carbon target in a solvent by means of laser pulses,[16,17] polyynes with extremely low fraction of by-products can be synthesized. During recent years, many research groups, intending to produce polyynes *via* PLAL, have employed ns-laser pulses. A few works based on ablation in water reported the synthesis of H-polyynes only up to H-C_{12}-H (for simplicity called hereafter C_{12}).[18–20] Matsutani *et al.*, instead, presented the ablation of perylene derivative, *i.e.* PCDTA, and a graphite pellet in different alcohols (methanol, ethanol, 1-propanol, 1-butanol, *t*-butyl alcohol) at 532 nm, obtaining polyynes with a length of 18 atoms.[21,22] They also reported the formation of C_{22} by irradiating graphite and fullerene suspension in *n*-hexane at a laser wavelength of 532 nm. The longest hydrogen-capped polyynes ever obtained *via* PLAL, C_{30}, have been obtained employing decalin at 1064 nm.[23,24] In addition to H-polyynes, another two sequences of sp-carbon chains detected by ablating the graphite target in acetonitrile were cyanopolyynes, *i.e.* H-C_n-CN (n = 6, 8, 10, 12), reported in the paper of Wakabayashi *et al.*[25] and dicyanopolyynes, NC-C_n-CN (n = 4, 6), found by Forte *et al.*[19] Moreover, polyynes capped by a methyl-group, *i.e.* H-C_n-CH_3 (n = 8, 10, 12), were synthesized in hexane[26] and in toluene, employing a fs-laser at the meniscus of the liquid.[27] Nevertheless, no systematic studies of the effect

Department of Energy, Politecnico di Milano, Via Ponzio 34/3, 20133, Milano, Italy. E-mail: carlo.casari@polimi.it

† Electronic supplementary information (ESI) available. See DOI: 10.1039/d0cp04132g

of different solvents on the properties of polyynes, *e.g.* yield, size and terminations, during PLAL experiments have been performed at the same fluence, wavelength and liquid volume (see Table S1 in the ESI†).

The solutions obtained after the ablation have been commonly studied *via* UV-vis spectroscopy, from which the polyyne concentration can be extracted.[9,28] High-performance liquid chromatography (HPLC) can be employed to separate in lengths and terminations the sp-carbon chains, allowing the characterization and collection of size-selected polyynes.[29] Moreover, Raman spectroscopy allows sp-hybridized linear carbon chains to be recognized because of their CC stretching mode in the frequency range of 1800–2200 cm^{-1}, where no peaks related to other functional groups are present.[30,31] Simulated and experimental Raman spectra show redshifts in correspondence with a longer chain length due to the increase of the conjugation.[32,33] Weak or undetectable Raman signals can be due to low concentrated samples or to strong luminescence signals, probably linked to the by-products of PLAL.[33] In this case, it is possible to use noble metal nanoparticles to enhance the sensitivity of the Raman signals up to six orders of magnitude by carrying out surface-enhanced Raman spectroscopy (SERS) measurements.[32] Despite the interest in analysing polyynes with different end-caps, no one to the best of our knowledge, examined the SERS of size-selected polyynes with terminations different from hydrogen produced by physical synthesis methods.

One of the major issues of polyynes is their poor stability, as they tend to rearrange in more stable sp^2-based structures *via* crosslinking reactions.[34] Only a few works discussed the evolution in time of polyynes in liquid solutions without silver nanoparticle colloids: the study of Cataldo after submerged arc discharge in acetonitrile[13] and the one of Compagnini and Scalese using water during PLAL.[35] Thus, to use sp-carbon chains in future applications, there is a need to understand how to obtain stable structures using a physical method, such as PLAL. In this framework, there are still some open questions regarding the solvent effect in determining the polyyne production yield, in providing specific terminating functional groups and in affecting the stability of polyynes in liquid.

We here provide a systematic investigation of the synthesis of polyynes *via* PLAL in different solvents, such as water, acetonitrile, ethanol, methanol and isopropanol, to outline their role in providing terminations for polyynes. UV-vis spectroscopy, HPLC and theoretical simulations have allowed us to recognize polyynes with lengths and terminations never reported so far in those solvents (*e.g.* C_{22} in organic solvents and methylpolyynes in all the selected solvents). SERS spectra have been obtained from size-selected and termination-selected polyynes. The specific stability of each type of polyyne has been investigated by analysing time constants for different lengths, terminations and solutions. Different solvent properties including polarity, composition, and oxygen dissolved are shown to compete in polyyne formation and behaviour, thus underlying the complex role of the solvent and the peculiar physical-chemistry of polyynes in liquid environments.

2 Experimental details

Polyynes were synthesized *via* pulsed laser ablation in liquid (PLAL) of a graphite target with a purity of 99.99% (Testbourne Ltd), using pulses from the second harmonic (λ = 532 nm) of a Nd:YAG pulsed laser (Quantel Q-smart 850) operating at a frequency of 10 Hz with a pulse duration of 6 ns. Ablation was performed for a fixed duration of 15 minutes in 2 mL of different solvents: deionised water Milli-Q (0.055 μS), acetonitrile (ACN), isopropanol (IPA), methanol (MeOH) and ethanol (EtOH) (Sigma-Aldrich, purity $\geq$ 99.9%). The laser beam was focused on the target with a lens having a 200 mm focal length and a fluence of 2.8 J cm^{-2} for all solvents (the effect of the liquid layer was taken into account in the calculations of the fluence[36]). During ablation, the sample holder stage was moved along a spiral path to ensure uniform ablation of the graphite target.

The ablated solutions were all filtered through Phenomenex Phenex RC-membrane syringe filters having a pore size of 0.45 μm to remove any sizeable impurities. The presence and concentration of polyynes were evaluated *via* UV-vis absorption spectroscopy (Shimadzu UV-1800 UV/visible Scanning Spectrophotometer with a 190–1100 nm spectral range). The optical path of the employed quartz cuvettes is 10 mm. To avoid signal saturation, samples were diluted in the proportion of 1/6 v/v for ablation in water and 1/60 v/v for the other solvents. Moreover, we analysed the UV-vis spectra from 340 nm to 210 nm due to the high absorption of the organic solvents below 210 nm.[37]

Reverse-phase high-performance liquid chromatography (RP-HPLC) was performed by means of a Shimadzu Prominence UFLC, equipped with a photodiode array (DAD) UV-vis spectrometer, an FRC-10A fraction collector and a C8 HPLC column (Shimadzu Shim-pack HPLC packed column GIST, 250 mm × 4.6 mm, 5 μm particle size). The detection of size- and termination-selected polyynes was achieved using a gradient elution: in this regime, the mobile phase initially consists in a solution of acetonitrile/water 50/50 v/v that gradually evolves to 90/10 v/v in 18 minutes. The overall analysis time was set to 60 min, with a constant flow rate of 1 mL min^{-1}. To estimate the stability of polyynes, we performed HPLC analysis at definite time intervals, until reaching 30 days, and we evaluated their degradation from the area under the chromatographic peaks associated to each polyyne. During the analysis period, the samples were stored in closed glass vials at room temperature in the dark. In addition, size-selected polyynes can be selectively collected for SERS investigations, for which the acetonitrile/water relative concentration depends on the collection time.

SERS spectra were collected using a Renishaw inVia Raman microscope with a diode-pumped solid-state laser (λ = 660 nm). Silver colloids (10^{-3} M) were synthesized following the Lee–Meisel method,[38] showing an absorption peak at 413 nm and a predicted mean diameter of $\sim$41 nm.[39] Silver colloids were added to size-separated polyynes 1/4 v/v to implement SERS analysis in liquid. The laser power was set to 75 mW during all measurements.

Density functional theory (DFT) simulations were performed on single linear chains using Gaussian09.[40] Time dependent density functional theory (TD-DFT) calculations were carried out for the prediction of the vibronic spectra at the CAM-B3LYP/cc-pVTZ level of theory, while PBE0/cc-pVTZ calculations were used for the computation of the Raman spectra. Based on TD-DFT calculations, Huang–Rys factors and vibronic spectra were computed using home-made programs.[41,42] The computed vibrational frequencies were multiplied by a scale factor of 0.961 in comparison with experimental spectra.[43] The choice of different functionals to compute the UV-vis or Raman spectra is related to the different accuracy of these functionals in computing these properties. Indeed, as known from the literature and as also discussed in our previous work,[42] vibronic spectra computed with CAM-B3LYP showed a very good agreement with the experimental ones, predicting their correct trend as a function of chain length. On the other hand, PBE0 overestimated π-conjugation effects for longer and longer chains, resulting in a less accurate description of the vibronic spectra. When vibrational spectra are considered, differently from CAM-B3LYP, PBE0 provides a very good agreement with experiments.[2,44]

3 Results and discussion

3.1 Characterization of polyyne structures

UV-vis absorption spectra of solutions prepared *via* pulsed laser ablation of graphite in acetonitrile, isopropanol, ethanol, methanol and pure water are shown in Fig. 1a. All the ablations were performed employing the same experimental parameters (laser fluence and wavelength, ablation time, solvent volume) to evaluate the effect of the solvent in the formation of polyynes. Each spectrum presents several peaks assigned to polyynes of different lengths. Specifically, in all the spectra the 0–0 band of the $^1\Sigma_u^+ \leftarrow X\ ^1\Sigma_g^+$ transition of the hydrogen-capped polyyne can be seen at 225 nm (C_8) and for the organic solvents at 251 nm (C_{10}), 275 nm (C_{12}), 295 nm (C_{14}) and 314 nm (C_{16}). The solutions in organic solvents are yellowish with a colour intensity varying from brown yellow for acetonitrile to pale yellow for methanol and fully transparent for water, in agreement with the absorption spectra (see the inset of Fig. 1). The spectra show an unresolved absorption background, related to the possible formation of hydrocarbons during the synthesis of polyynes. Such a background monotonically decreases with wavelength, as observed by Taguchi and co-workers.[9,28] The spectra, after the subtraction of the background obtained by fitting the baseline with decreasing exponential and the polyyne peaks with Gaussian curves, are presented in Fig. 1b. The polyyne production yield was estimated from the absorbance values extracted from Fig. 1b by calculating χ_p, which represents the "index of purity" in the previous works of Taguchi and co-workers.[9,28] It is defined as the ratio between the integrated absorption of the 0–0 band of the $^1\Sigma_u^+ \leftarrow X\ ^1\Sigma_g^+$ transition of H-polyynes to that of the fitted background of hydrocarbon by-products.[9] The lowest χ_p was found in the case of water with

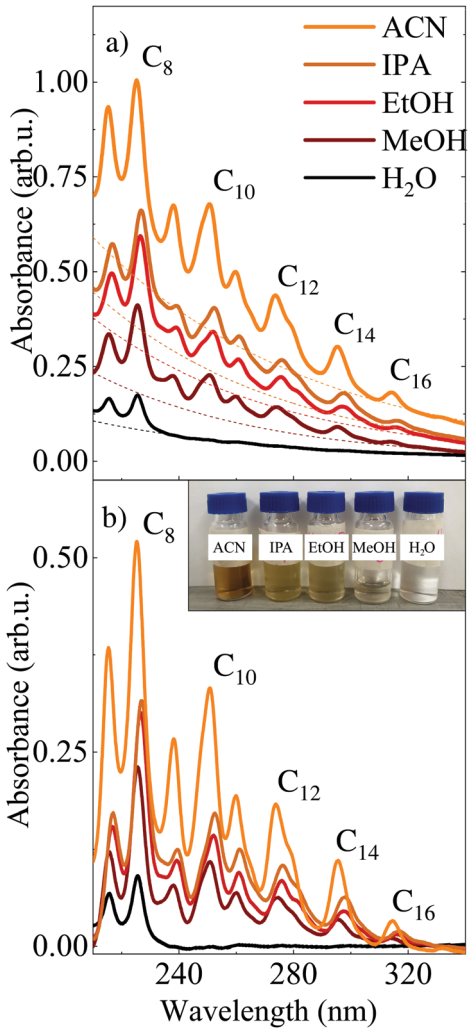

Fig. 1 UV-vis spectra of filtered solutions of polyynes in acetonitrile, isopropanol, methanol, ethanol and water after laser ablation before (a) and after (b) the background (dotted lines) subtraction. The 0–0 band of the $^1\Sigma_u^+ \leftarrow X\ ^1\Sigma_g^+$ transition of the hydrogen-capped polyynes with lengths of 8, 10, 12, 14, and 16 carbon atoms are, respectively, referred to as C_8, C_{10}, C_{12}, C_{14}, and C_{16}. Pictures of the different solutions are presented in the inset.

a value of 0.0749 ± 0.0001 and the highest "purity" of polyynes over the other contaminants was observed in methanol at 0.3015 ± 0.0003, followed by isopropanol at 0.2860 ± 0.0043, ethanol at 0.2766 ± 0.0035 and acetonitrile at 0.2057 ± 0.0005. The values of χ_p have been plotted as a function of the solvent polarity (see Fig. 2), considering a value of 100 for the polarity of water. The polyynes concentration in each solvent (see Table S2 in the ESI†) has been reported in the same picture and it has been evaluated using the Lambert–Beer law, employing molar extinction coefficients taken from the literature.[6] We observe that the polyyne concentration decreases with increasing the polarity of the solvents in agreement with previous works,[21,45] whereas, apart from water, we observe an opposite behaviour for the χ_p value, which is larger with a lower polyyne concentration.

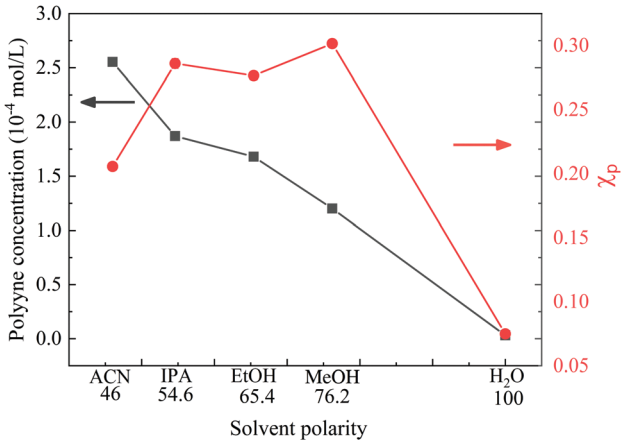

Fig. 2 Overall polyyne concentration (mol L^{-1}) and χ_p as a function of the solvent polarity.

Polyynes, which are nonpolar molecules and liable to oxidation,[10] are more concentrated in acetonitrile probably because the solvent has the lowest polarity[46] and the smallest quantity of dissolved oxygen compared to the other solvents (see Table S2 in the ESI† for the values of oxygen present in the other solvents).[47] Moreover, acetonitrile has a higher tendency towards carbonization with respect to alcohols.[48] Indeed, alcohols contain oxygen and are characterized by H/C ratios of 0.33 for MeOH, 0.4 for EtOH, and 0.5 for IPA, which are lower than that of ACN (*i.e.* 0.66). The coking reaction could give a secondary source of carbon species in the plasma phase[25,49] but, in parallel, it causes the formation of hydrocarbons, which affects the χ_p value. For these reasons, the solution of polyynes synthesized in acetonitrile, despite the high concentration, turns out to be characterized by a lower value of χ_p compared to alcohols, corresponding to the larger hydrocarbon-correlated background, as mentioned before.[48] In the case of water, we observe the lowest concentration of polyynes and the smallest value of χ_p, thus exhibiting the worst yield of polyynes. This result can be explained considering that water does not contribute to provide carbon atoms for the polyyne formation process[25] and its hydrogen generation rate, which is an important factor in polyyne formation,[17,50] is the lowest one with respect to the organic solvents. In fact, the H–OH bond in water (4.8 eV) is less likely to break than the molecular bonds in organic liquids, such as C–H (4.3 eV), C–C (3.6 eV) and C–O (3.7 eV).[51,52]

HPLC allows detailed investigation of the length and termination of the polyynes present in the samples. After processing the data obtained from the DAD coupled with HPLC, a 2D graph of absorbance as a function of time and wavelength shows the presence of different polyyne species eluted between 10 and 32 minutes in acetonitrile solution (see Fig. 3a). All the corresponding times on the chromatogram and the positions of the experimental, simulated and published UV-vis absorption peaks are reported in Table S3 in the ESI,† together with related references of previous investigations.[23,25–27,42] We detected nine different species of hydrogen-capped polyynes ranging from 6 to 22 sp-carbon atoms, the UV-vis spectra of which are presented in Fig. 3b. The same size of H-polyynes was found also in the case of methanol, ethanol and isopropanol at analogous times as those in acetonitrile. The species C_6 was previously not discussed because its UV-vis absorption peaks fall in the UV cut-off region of the alcohols. Moreover, we individuated other types of sp-carbon wires, which we attributed to polyynes terminated with methyl (H-C_n-CH_3) and cyano (H-C_n-CN) groups, thanks to a multi-technique characterization based on experimental and computed data, as discussed later in this section. The corresponding UV-vis spectra are presented in Fig. 3c and d. Cyanopolyynes were obtained only *via* laser ablation in acetonitrile, while methylpolyynes were noticed also *via* ablation in all the other solvents, including water. In the last case, we unexpectedly noticed a methylpolyyne, *i.e.* HC_8CH_3, while in all the other organic solvents we found the methylpolyynes identified in Fig. 3c. The development of an optimized HPLC separation method (see Section 2), which is able to differentiate two very similar constituents, allowed cyano- and methyl-polyynes to be distinguished from H-polyynes. To confirm our assignments, we first considered the times at which the species were eluted using the chromatographic system (see Fig. 3a and Table S3 in the ESI†). Each peak appeared on the chromatogram according to the size of the polyyne molecules. We observed, between the peaks of two neighbouring hydrogen-capped polyynes, the presence of cyanopolyynes, followed by methylpolyynes, which both have the same number of sp-carbon atoms. When molecules are characterized by analogous dimension, the driving factor for their separation is their polarity: highly polar molecules are less retained by the HPLC column.[53] For this reason, cyanopolyynes, which are more polar than methylpolyynes, were eluted first, as shown in Fig. 3a. Secondly, to support the interpretation of our UV-vis data, we performed TD-DFT simulations to compute vibronic spectra. The predicted data were rigidly shifted to match the spectra of C_8, considered as a reference system as in our previous work.[42] Transition energies are well described using the TD-DFT model, even if, by increasing the length of the chain, the discrepancy with respect to the experimental values increases. This effect can be due to the partial multireference behaviour of the polyyne excited states not considered in TD-DFT.[42] Finally, we observe a good agreement between the experimental main UV absorption peaks and those reported in the literature, except for small shifts of approximately 2–3 nm in some cases due to the specific liquid environment.[54] Similar chain lengths were reported in previous works for hydrogen-capped polyynes *via* ablation in solvents such as hexane, *n*-hexane and decalin[23,24,55,56] and for cyanopolyynes *via* ablation in acetonitrile,[19,25] while only methyl-capped polyynes, *i.e.* with n = 10, 12, 14 were discussed in the literature.[26,27] Our results suggest the formation of other methyl-capped polyynes with n = 6, 8, 16, and 18 and show the detection of a methyl-capped polyyne in water for the first time, *i.e.* with n = 8.

Polyynes of the same size and different terminations have been investigated *via* Raman spectroscopy. Using HPLC, we separated and collected the species with 8 sp-carbon atoms, namely C_8, H-C_8-CH_3 and H-C_8-CN. We used this series as a

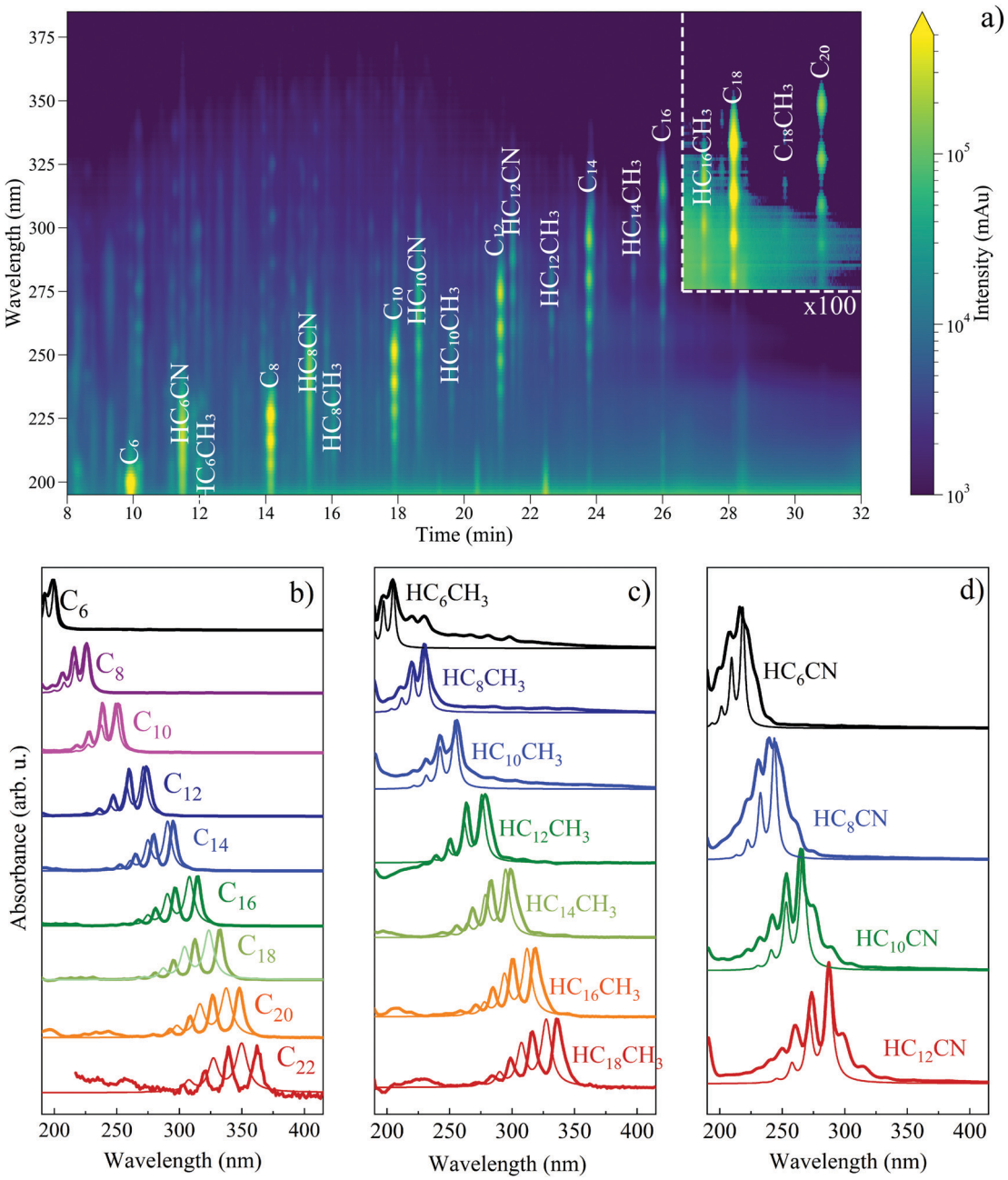

Fig. 3 (a) 2D graph of the absorbance as a function of wavelength and the time extracted from DAD coupled with the HPLC system. Normalized experimental (thick lines) and simulated (thin lines) UV-vis spectra of (b) H-polyynes, (c) CH_3-polyynes and (d) CN-polyynes obtained after the ablation of the graphite target in acetonitrile.

benchmark due to its high concentration and stability, which allows us to efficiently separate them. The low concentration of polyynes ($\lesssim 10^{-4}$ M) and the lower Raman activity of short polyynes, compared to the longer ones, resulted in a too weak Raman signal, which needed to be enhanced *via* the SERS technique.[33] Hence, we added silver colloids to perform SERS in liquids of the three species as shown in Fig. 4. We notice two main broad bands below and above 2000 cm^{-1} in all three measurements. The band below 2000 cm^{-1} usually appears in the SERS spectra of polyynes, as reported in many works,[32,33,57] whereas the band at a higher wavenumber corresponds to the ECC mode of sp-carbon chains, consisting of a collective vibration of the CC bonds, specifically the C≡C stretching and C–C shrinking mode.[58] Concerning the ECC mode, we observe in Fig. 4 a nearly symmetrical peak at 2079 cm^{-1} in C_8, a band centred at 2073 cm^{-1} in H-C_8-CH_3 and a doublet in H-C_8-CN, for which the most intense peak is located at 2067 cm^{-1} and a secondary one at 2093 cm^{-1}. Such differences in the shape and position of the ECC band are due to the modulation of polyyne conjugation and possibly to the preferential interaction of silver nanoparticles with the different ends of the chains.[32] In fact, methyl-capped and cyano-capped polyynes

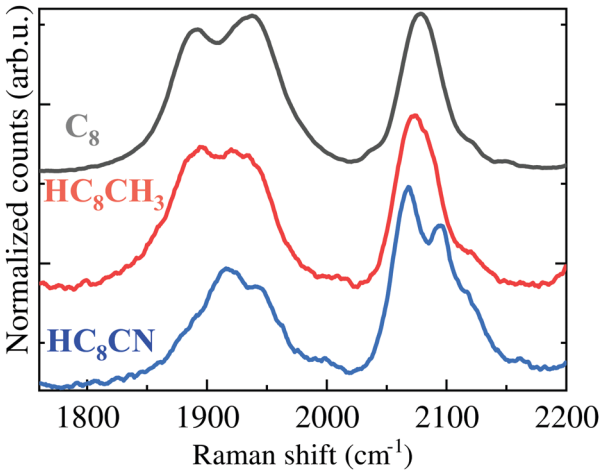

Fig. 4 Normalized experimental SERS spectra of liquid solutions of size-selected polyynes with four triple bonds H–(C≡C)$_4$– and different end-caps (–H/–CH$_3$/–CN). The curves related to methyl- and cyano-capped polyynes were smoothed in order to better individuate the sp Raman features.

present at one end different end-groups, which contribute to an increase in π-conjugation. The CH_3 group can give charge to the sp-chain due to a hyperconjugation effect,[59–61] while the CN group takes part in the π-electron delocalization due to the presence of the sp orbital of the N atom. This explains the red shift from C_8 (2079 cm^{-1}), to H-C_8-CH_3 (2073 cm^{-1}), to H-C_8-CN (2067 cm^{-1}).[58] The general trend of the relative positions of these peaks is also shown by simulated Raman spectra of a single molecule without Ag nanoparticles presented in Fig. S1a in the ESI.† A mismatch between simulated and experimental peak positions is observed due to the interaction with silver colloids that is not included in our calculations.[32,33,57] However, the unpredicted anomalous double-peaked band in the SERS spectra of H-C_8-CN is probably due to the interaction of silver nanoparticles with two possible adsorption sites, namely H and CN.[33,62] We do not observe the same splitting effect in H-C_8-CH_3 because we expect the methyl-group to contribute only slightly in the collective vibrational mode due to its sp^3 nature (see Fig. S1b in the ESI†). The aforementioned asymmetry of the ECC band can be an indication of a different interaction with silver nanoparticles in the possible different sites of the molecule, which affects the ECC mode to a minor extent. In this picture, the symmetric band of C_8 can be related to the presence of two identical terminations as interaction sites with Ag nanoparticles. Even though further computational calculations with suitable models should be developed to analyse more deeply the origin of the experimental SERS spectra, SERS appears to be sensitive to the chain termination showing its potential in the investigation of polyynes.

3.2 Mechanism of formation

As described in the previous section, we identified and characterized hydrogen-, methyl- and cyano-terminated polyynes. How different atoms or molecular groups can form at the terminations of the sp-carbon chains during the PLAL process is a non-trivial issue. We here provide some considerations to discuss the possible mechanism of formation of polyynes during the PLAL process. It is known that sp-carbon chains obtained *via* laser ablation of a carbon-based target can be formed at the plume shock front, where strong out-of-equilibrium conditions, characterized by high pressure and temperature gradients, occur. In the PLAL process, the plasma is rapidly quenched by the liquid, which cools down the vapour, confines the species formed in a small volume and favours clustering.[49] A similar phenomenon takes place during nanosecond pulsed laser deposition (PLD) in a background gas or in supersonic cluster beam sources, such as laser vaporization and pulsed microplasma cluster sources.[63,64] In these methods, the background gas plays a similar role of the liquid in quenching and confining the plasma, and in favouring clustering of the ablated species. In fact, it was shown that ns-PLD without any liquid or gaseous environment, *i.e.* in vacuum, cannot produce sp-carbon chains. The fundamental role of a strong confining medium in nanosecond ablation is thus evident by the high background gas pressure needed to observe polyyne formation (*i.e.* 500 Pa) and confirms that a liquid medium can provide optimal conditions for the growth of sp-carbon structures. In particular, the synthesis of polyynes seems to take place in a specific time-window, sufficiently long to cool down the carbon vapour, but short enough to avoid the degradation of sp-carbon into more stable sp^2 hydrocarbons. Indeed, the species produced close to the ablation region are too hot to be terminated and need to move far from the region where the plasma plume originates.[9,63] The existence of appropriate conditions for polyyne formation is supported by the work of Cannella and Goldman, reporting the simulation of graphite liquid phase, obtained *via* laser melting at 5000 K.[65] Once proper conditions of pressure, temperature and time are reached in the ablation process, polyynes can grow through the addition of carbon dimers and/or ethynyl radicals.[16,18] This results in the formation of polyynes rapidly decreasing with increasing length, as also confirmed by our HPLC analysis. In PLAL, the role of solvent turns out to be crucial in the formation of sp-carbon chains and has a two-fold function: to act as a carbon source and to provide chain terminations.[25,52] The first is evident from the larger formation yield of polyynes produced in organic solvents compared to the case of water (see Table S2 in the ESI†). The second is highlighted by the different kinds of terminations found in this work, which strictly depends on the solvent functional groups. Indeed, the high plasma temperature may induce direct degradation, ionization and pyrolysis of the liquid into atomic or molecular radicals.[49,52] This causes the formation of different redox equivalents including carbon-based radicals and hydrogen,[52] which may terminate the growing chain, as in the case of hydrogen-capped polyynes.[9,16] This phenomenon can be applied to the other terminations observed in this work. For example, the formation of cyano-capped polyynes is evidently driven by the presence of acetonitrile and indicates the production of cyano-molecular radicals able to terminate carbon-atom wires. The same mechanism may occur to

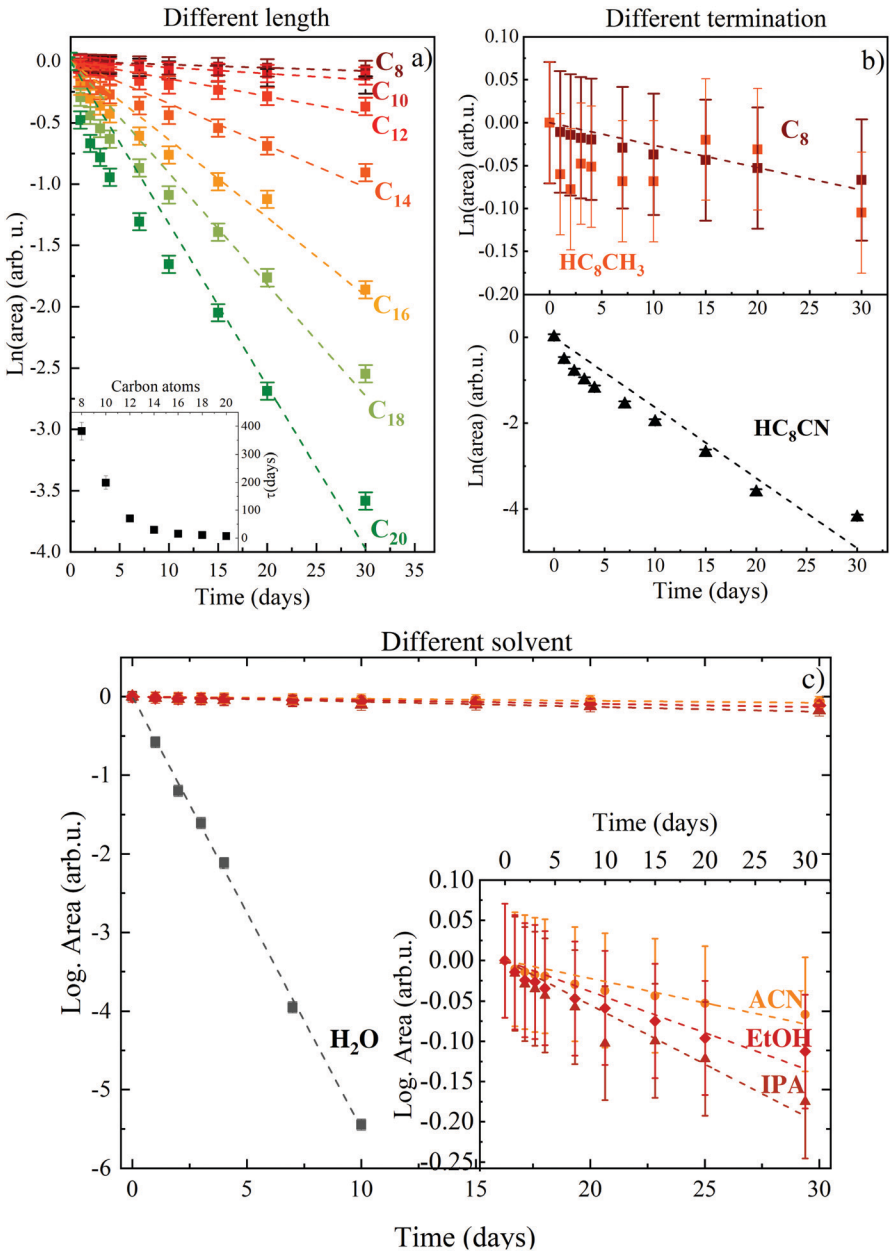

Fig. 5 Reduction in time of the chromatographic peak area of polyynes under specific parameters. (a) Effect of the chain length from n = 8 to 20. Inset: Decay time constant (τ) for each polyyne. (b) Effect of the terminations: −H, $-CH_3$ and −CN. (c) Effect of the solvents on C_8 such as water, acetonitrile, isopropanol, and ethanol. Inset: Magnification of polyyne solutions in organic solvents. The decay time constants are reported in Table S4 in the ESI.†

methyl-capped polyynes in all the organic solvents. Remarkably, we also observed their formation in water, suggesting that methyl-groups may terminate the chains through the binding of three hydrogen radicals at one end. However, this process occurs with a very low probability, since, from the HPLC data, the concentration of methyl-capped polyynes in water is two orders of magnitude lower than that of hydrogen-capped ones (see Fig. S2 in the ESI†).

3.3 Stability of polyynes

We investigated the ageing in time of polyynes as a function of their size and termination. It is known that the degradation of sp-carbon chains is mainly due to the exposure to oxidising agents and to crosslinking interactions.[34,66] Here, we have been studying the effect of some factors on polyyne stability, *e.g.* chain lengths, terminations and solvents. We extracted the decay time constants monitoring the solutions of polyyne mixture for 30 days *via* periodic HPLC analysis, keeping them in closed vials and under room conditions. From each measurement, we estimated the amount of selected polyynes at specific times using their chromatographic peak area (A_t) and compared it with the area of the as-prepared solution (A_0). The experimental data and the corresponding error bar of 5%, due to the HPLC apparatus, are presented in Fig. 5. In some cases, the temporal evolution of $\ln(A_t/A_0)$ is well described by a linear

fitting, from which we calculated the characteristic decay time constants, τ. We show in Fig. 5a the area reduction of size-selected H-polyynes synthesized in acetonitrile, revealing that shorter polyynes are more stable than longer ones, as highlighted by the values of τ as a function of the number of carbon atoms (see inset), as previously discussed by Cataldo.[13] In fact, the shortest polyyne herein reported, *i.e.* C_8, has a decay time constant of 382 days, which is 50 times slower than the longest one (7.6 days), *i.e.* C_{20}, and 4 times greater than C_{14} (29 days) (see Table S4 in the ESI†). In Fig. 5b, for a fixed length of 8 sp-carbon atoms, we compare the different terminations in acetonitrile solution: hydrogen-terminated polyyne (C_8), methyl (HC_8CH_3) and cyano (HC_8CN) as terminating groups. HC_8CH_3 displays a similar evolution in time to C_8 but with more fluctuations, so the linear fitting could not be performed. We can justify this behaviour considering the steric hindrance of the methyl-group, which may reduce the probability of cross-linking reactions between sp-carbon chains, while fluctuations can be due to the low concentration of HC_8CH_3 present in the solution. Furthermore, HC_8CN has a decay time constant of 6 days, which is two orders of magnitude lower than that of hydrogen-capped polyynes, as already observed by Cataldo.[13] Specifically, this happens because cyanopolyynes, being more reactive than hydrogen-ended ones, oxidise first.

To investigate the effect of the chemical environment on polyyne stability, we present in Fig. 5c the temporal evolution of the chromatographic peak area of the most stable size-selected polyyne, *i.e.* C_8, in water and organic solvents. Polyynes are not very stable in water due to their low solubility and non-polarity, as previously discussed. In fact, C_8, whose τ in water is about 1.8 days, was not anymore detected *via* HPLC after 10 days. Instead, its decay time constants in all the organic solvents such as acetonitrile (382 days), isopropanol (156 days) and ethanol (224 days), are two orders of magnitude higher than those in the case of water (*i.e.* 1.8 days) and exhibit only small differences during the analysis period. In fact, the chromatographic peak area of C_8 in ACN is decreased by 6% after 30 days, whereas, for EtOH and IPA, the reduction is, respectively, up to 11% and 16%. These data can be explained by considering the increased solubility of polyynes in organic solvents as compared with water, due to their lower polarity. Furthermore, ACN, EtOH and IPA have higher χ_p, which causes the formation of a lower amount of by-products that can interact with polyynes leading to degradation. Considering the liquid environments investigated, the fact that acetonitrile ensures the better stability of polyynes than the others can be linked to its minimal value of polarity and the slightest quantity of oxygen dissolved in the solvent[47] (see Ostwald coefficients in Table S2 in the ESI†), responsible for the oxidation of the chains.[13] EtOH ensures a slightly greater stability than IPA presumably because, at the same χ_p, the quantity of oxygen present per volume of solvent is lower. When increasing the length of H-polyynes, we observe the same trend with respect to the solvents. Regarding the methyl-capped polyynes, we notice an irregular behaviour with fluctuations in the order of the experimental error, already demonstrated in Fig. 5b, not only in ACN but also in IPA and EtOH. In conclusion, the obtained results showed that organic solvents improved the stability of polyynes compared to water, confirming the enhanced stability observed when acetonitrile was added to the aqueous solution of polyynes.[42]

4 Conclusions

We demonstrated the effect of different solvents on the efficiency of the formation of polyynes and their stability. Specifically, we have considered water, acetonitrile, methanol, ethanol and isopropanol as solvents. H-polyynes up to C_{22} could be separated *via* HPLC in all the solvents investigated here, except for water. The presence of cyano- and methyl-polyynes was observed *via* UV-vis spectroscopy, also supported through a comparison with the literature and TD-DFT simulations. The SERS spectra of isolated size-selected polyynes with the three terminations C_8, HC_8CH_3 and HC_8CN revealed the differences in the position and shape of the SERS bands in the sp-carbon range. In addition, we investigated the evolution in time of the polyynes considering the role of the chain length, terminations, and solvents. In conclusion, the degradation in time of short hydrogen-capped polyynes was well described by a decaying exponential and acetonitrile provided different advantages: the high concentration of sp-carbon chains during the laser ablation of graphite, the coexistence of three series of polyynes and a larger stability for H-polyynes with respect to the other solvents investigated. The possibility to use the participating solvents in the PLAL of graphite allows the synthesis of polyynes with different termination openings for the modulation of their properties *via* selection of the size and type of end group.

Conflicts of interest

There are no conflicts to declare.

Acknowledgements

The authors acknowledge funding from the European Research Council (ERC) under the European Union's Horizon 2020 research and innovation program ERC-Consolidator Grant (ERC CoG 2016 EspLORE grant agreement no. 724610, website: www.esplore.polimi.it).

References

1 C. Casari and A. Milani, *MRS Commun.*, 2018, **8**, 207–219.
2 C. S. Casari, M. Tommasini, R. R. Tykwinski and A. Milani, *Nanoscale*, 2016, **8**, 4414–4435.
3 A. L. K. Shi Shun and R. R. Tykwinski, *Angew. Chem., Int. Ed.*, 2006, **45**, 1034–1057.
4 W. Duley and D. Williams, *Mon. Not. R. Astron. Soc.*, 1984, **211**, 97–103.
5 J. August, H. W. Kroto and N. Trinajstic, *Astrophys. Space Sci.*, 1986, **128**, 411–419.

6 R. Eastmond, T. Johnson and D. Walton, *Tetrahedron*, 1972, **28**, 4601–4616.
7 F. Cataldo, *Carbon*, 2003, **41**, 2671–2674.
8 W. A. Chalifoux and R. R. Tykwinski, *Nat. Chem.*, 2010, **2**, 967–971.
9 Y. Taguchi, H. Endo, Y. Abe, J. Matsumoto, T. Wakabayashi, T. Kodama, Y. Achiba and H. Shiromaru, *Carbon*, 2015, **94**, 124–128.
10 F. Cataldo, *Fullerenes, Nanotubes, Carbon Nanostruct.*, 2004, **12**, 603–617.
11 F. Cataldo, *Fullerenes, Nanotubes, Carbon Nanostruct.*, 2004, **12**, 619–631.
12 F. Cataldo, *Fullerenes, Nanotubes, Carbon Nanostruct.*, 2004, **12**, 619–631.
13 F. Cataldo, *Fullerenes, Nanotubes, Carbon Nanostruct.*, 2007, **15**, 155–166.
14 F. Cataldo, *Tetrahedron*, 2004, **60**, 4265–4274.
15 Y. Wu, Y. Zhang, T. Zhu, H. Li, Y. Liu and X. Zhao, *Chem. Phys. Lett.*, 2019, **730**, 64–69.
16 M. Tsuji, T. Tsuji, S. Kuboyama, S.-H. Yoon, Y. Korai, T. Tsujimoto, K. Kubo, A. Mori and I. Mochida, *Chem. Phys. Lett.*, 2002, **355**, 101–108.
17 M. Tsuji, S. Kuboyama, T. Matsuzaki and T. Tsuji, *Carbon*, 2003, **41**, 2141–2148.
18 G. Compagnini, V. Mita, R. S. Cataliotti, L. DUrso and O. Puglisi, *Carbon*, 2007, **45**, 2456–2458.
19 G. Forte, L. DUrso, E. Fazio, S. Patanè, F. Neri, O. Puglisi and G. Compagnini, *Appl. Surf. Sci.*, 2013, **272**, 76–81.
20 G. Grasso, L. DUrso, E. Messina, F. Cataldo, O. Puglisi, G. Spoto and G. Compagnini, *Carbon*, 2009, **47**, 2611–2619.
21 R. Matsutani, T. Kakimoto, H. Tanaka and K. Kojima, *Carbon*, 2011, **49**, 77–81.
22 R. Matsutani, T. Kakimoto, K. Wada, T. Sanada, H. Tanaka and K. Kojima, *Carbon*, 2008, **46**, 1103–1106.
23 R. Matsutani, K. Inoue, T. Sanada, N. Wada and K. Kojima, *J. Photochem. Photobiol., A*, 2012, **240**, 1–4.
24 R. Matsutani, K. Inoue, N. Wada and K. Kojima, *Chem. Commun.*, 2011, **47**, 5840–5842.
25 T. Wakabayashi, M. Saikawa, Y. Wada and T. Minematsu, *Carbon*, 2012, **50**, 47–56.
26 Y. Wada, K. Koma, Y. Ohnishi, Y. Sasaki and T. Wakabayashi, *Eur. Phys. J. D*, 2012, **66**, 322.
27 A. Ramadhan, M. Wesolowski, T. Wakabayashi, H. Shiromaru, T. Fujino, T. Kodama, W. Duley and J. Sanderson, *Carbon*, 2017, **118**, 680–685.
28 Y. Taguchi, H. Endo, T. Kodama, Y. Achiba, H. Shiromaru, T. Wakabayashi, B. Wales and J. Sanderson, *Carbon*, 2017, **115**, 169–174.
29 *Polyynes*, ed. F. Cataldo, CRC Press, 2005.
30 J. Kūrti, C. Magyar, A. Balázs and P. Rajczy, *Synth. Met.*, 1995, **71**, 1865–1866.
31 *Carbyne and Carbynoid Structures*, ed. R. B. Heimann, S. E. Evsyukov and L. Kavan, Springer, Netherlands, 1999.
32 A. Lucotti, M. Tommasini, M. D. Zoppo, C. Castiglioni, G. Zerbi, F. Cataldo, C. Casari, A. L. Bassi, V. Russo, M. Bogana and C. Bottani, *Chem. Phys. Lett.*, 2006, **417**, 78–82.
33 H. Tabata, M. Fujii, S. Hayashi, T. Doi and T. Wakabayashi, *Carbon*, 2006, **44**, 3168–3176.
34 C. S. Casari, A. Li Bassi, L. Ravagnan, F. Siviero, C. Lenardi, P. Piseri, G. Bongiorno, C. E. Bottani and P. Milani, *Phys. Rev. B: Condens. Matter Mater. Phys.*, 2004, **69**, 075422.
35 G. Compagnini and S. Scalese, *Laser Ablation in Liquids: Principles and Applications in the Preparation of Nanomaterials*, 2012, p. 439.
36 A. Menéndez-Manjón, P. Wagener and S. Barcikowski, *J. Phys. Chem. C*, 2011, **115**, 5108–5114.
37 A. Krstulovic and P. Brown, *Reversed Phase High-Performance Liquid Chromatography: Theory, Practice and Biochemical Applications*, Wiley, 1982.
38 P. C. Lee and D. Meisel, *J. Phys. Chem.*, 1982, **86**, 3391–3395.
39 D. Paramelle, A. Sadovoy, S. Gorelik, P. Free, J. Hobley and D. G. Fernig, *Analyst*, 2014, **139**, 4855.
40 M. J. Frisch, G. W. Trucks, H. B. Schlegel, G. E. Scuseria, M. A. Robb, J. R. Cheeseman, G. Scalmani, V. Barone, B. Mennucci, G. A. Petersson, H. Nakatsuji, M. Caricato, X. Li, H. P. Hratchian, A. F. Izmaylov, J. Bloino, G. Zheng, J. L. Sonnenberg, M. Hada, M. Ehara, K. Toyota, R. Fukuda, J. Hasegawa, M. Ishida, T. Nakajima, Y. Honda, O. Kitao, H. Nakai, T. Vreven, J. A. Montgomery, Jr, J. E. Peralta, F. Ogliaro, M. Bearpark, J. J. Heyd, E. Brothers, K. N. Kudin, V. N. Staroverov, R. Kobayashi, J. Normand, K. Raghavachari, A. Rendell, J. C. Burant, S. S. Iyengar, J. Tomasi, M. Cossi, N. Rega, J. M. Millam, M. Klene, J. E. Knox, J. B. Cross, V. Bakken, C. Adamo, J. Jaramillo, R. Gomperts, R. E. Stratmann, O. Yazyev, A. J. Austin, R. Cammi, C. Pomelli, J. W. Ochterski, R. L. Martin, K. Morokuma, V. G. Zakrzewski, G. A. Voth, P. Salvador, J. J. Dannenberg, S. Dapprich, A. D. Daniels, Ö. Farkas, J. B. Foresman, J. V. Ortiz, J. Cioslowski and D. J. Fox, *Gaussian09 Revision E.01*, Gaussian Inc., Wallingford CT, 2009.
41 W. Yang, G. Longhi, S. Abbate, A. Lucotti, M. Tommasini, C. Villani, V. J. Catalano, A. O. Lykhin, S. A. Varganov and W. A. Chalifoux, *J. Am. Chem. Soc.*, 2017, **139**, 13102–13109.
42 S. Peggiani, A. Senis, A. Facibeni, A. Milani, P. Serafini, G. Cerrato, A. Lucotti, M. Tommasini, D. Fazzi, C. Castiglioni, V. Russo, A. L. Bassi and C. S. Casari, *Chem. Phys. Lett.*, 2020, **740**, 137054.
43 R. D. Johnson III, NIST 101. Computational chemistry comparison and benchmark database, Nist technical report, 1999.
44 A. Milani, M. Tommasini, V. Russo, A. L. Bassi, A. Lucotti and F. Cataldo, *et al.*, *Beilstein J. Nanotechnol.*, 2015, **6**, 480–491.
45 Y. Zhang, T. Zhu, T. Maruyama, Y. Liu, H. Li, Y. Wu and X. Zhao, *Chem. Phys.*, 2020, **535**, 110804.
46 I. Smallwood, *Handbook of Organic Solvent Properties*, Elsevier Science, 2012.
47 G. R. R. Bebahani, P. Hogan and W. E. Waghorne, *J. Chem. Eng. Data*, 2002, **47**, 1290–1292.
48 F. Cataldo, *Tetrahedron*, 2004, **60**, 4265–4274.
49 V. Amendola and M. Meneghetti, *Phys. Chem. Chem. Phys.*, 2013, **15**, 3027–3046.

50 Y. E. Park, S. K. Shin and S. M. Park, *Bull. Korean Chem. Soc.*, 2012, **33**, 2439–2442.

51 J. Dean and N. Lange, *Lange's Handbook of Chemistry*, McGraw-Hill, 1999.

52 A. Kanitz, M.-R. Kalus, E. L. Gurevich, A. Ostendorf, S. Barcikowski and D. Amans, *Plasma Sources Sci. Technol.*, 2019, **28**, 103001.

53 L. Snyder, J. Kirkland and J. Dolan, *Introduction to Modern Liquid Chromatography*, Wiley, 2011.

54 A. Gillam and E. Stern, *An Introduction to Electronic Absorption Spectroscopy in Organic Chemistry*, E. Arnold, 1954.

55 R. Matsutani, F. Ozaki, R. Yamamoto, T. Sanada, Y. Okada and K. Kojima, *Carbon*, 2009, **47**, 1659–1663.

56 K. Inoue, R. Matsutani, T. Sanada and K. Kojima, *Carbon*, 2010, **48**, 4209–4211.

57 A. Lucotti, C. Casari, M. Tommasini, A. L. Bassi, D. Fazzi, V. Russo, M. D. Zoppo, C. Castiglioni, F. Cataldo, C. Bottani and G. Zerbi, *Chem. Phys. Lett.*, 2009, **478**, 45–50.

58 N. R. Agarwal, A. Lucotti, D. Fazzi, M. Tommasini, C. Castiglioni, W. Chalifoux and R. R. Tykwinski, *J. Raman Spectrosc.*, 2013, **44**, 1398–1410.

59 C. Castiglioni, M. Gussoni and G. Zerbi, *J. Mol. Struct.*, 1989, **198**, 475–488.

60 C. Castiglioni, M. Gussoni and G. Zerbi, *J. Mol. Struct.*, 1986, **141**, 341–346.

61 P. Jona, M. Gussoni and G. Zerbi, *J. Phys. Chem.*, 1981, **85**, 2210–2218.

62 G. E. Coates and C. Parkin, *J. Inorg. Nucl. Chem.*, 1961, **22**, 59–67.

63 C. Casari, C. Giannuzzi and V. Russo, *Carbon*, 2016, **104**, 190–195.

64 L. Ravagnan, F. Siviero, C. Lenardi, P. Piseri, E. Barborini and P. Milani, *Phys. Rev. Lett.*, 2002, **89**, 28–31.

65 C. B. Cannella and N. Goldman, *J. Phys. Chem. C*, 2015, **119**, 21605–21611.

66 M. Springborg and L. Kavan, *Chem. Phys.*, 1992, **168**, 249–258.